In vivo prevention of arterial restenosis with paclitaxel-encapsulated targeted lipid–polymeric nanoparticles

Juliana M. Chan[a,1], June-Wha Rhee[b,1], Chester L. Drum[c], Roderick T. Bronson[d], Gershon Golomb[e], Robert Langer[c,2], and Omid C. Farokhzad[b,2]

[a]Department of Biology, Massachusetts Institute of Technology, Cambridge, MA 02139; [b]Laboratory of Nanomedicine and Biomaterials, Department of Anesthesiology, Brigham and Women's Hospital, Harvard Medical School, Boston, MA 02115; [c]Department of Chemical Engineering and Division of Health Science and Technology, Massachusetts Institute of Technology, Cambridge, MA 02139; [d]Rodent Histopathology Core, Harvard Medical School, Boston, MA 02115; and [e]School of Pharmacy, Hebrew University of Jerusalem, Jerusalem 91120, Israel

Contributed by Robert Langer, October 2, 2011 (sent for review March 28, 2011)

Following recent successes with percutaneous coronary intervention (PCI) for treating coronary artery disease (CAD), many challenges remain. In particular, mechanical injury from the procedure results in extensive endothelial denudation, exposing the underlying collagen IV-rich basal lamina, which promotes both intravascular thrombosis and smooth muscle proliferation. Previously, we reported the engineering of collagen IV-targeting nanoparticles (NPs) and demonstrated their preferential localization to sites of arterial injury. Here, we develop a systemically administered, targeted NP system to deliver an antiproliferative agent to injured vasculature. Approximately 60-nm lipid–polymeric NPs were surface functionalized with collagen IV-targeting peptides and loaded with paclitaxel. In safety studies, the targeted NPs showed no signs of toxicity and a ≥3.5-fold improved maximum tolerated dose versus paclitaxel. In efficacy studies using a rat carotid injury model, paclitaxel (0.3 mg/kg or 1 mg/kg) was i.v. administered postprocedure on days 0 and 5. The targeted NP group resulted in lower neointima-to-media (N/M) scores at 2 wk versus control groups of saline, paclitaxel, or nontargeted NPs. Compared with sham-injury groups, an ∼50% reduction in arterial stenosis was observed with targeted NP treatment. The combination of improved tolerability, sustained release, and vascular targeting could potentially provide a safe and efficacious option in the management of CAD.

Percutaneous coronary interventions (PCIs) using drug-eluting stents (DESs) are credited with significant reductions in vessel restenosis, due to the effective combination of a drug delivery system and mechanical scaffold (1). Despite the extensive clinical use of DESs to maintain vascular patency, not all coronary lesions are amenable to DES placement (2). In addition, DESs are associated with delayed endothelialization (3) and increased thrombogenicity (4, 5) that require extended antiplatelet treatment (6). In some cases, only bare metal stents (BMSs) may be applied, which lack the benefit of antirestenotic therapy and instead stimulate neointimal smooth muscle cell (SMC) proliferation (7, 8).

Nanomedicines may offer improvements to existing clinical treatments, including those for cardiovascular disorders (9, 10). Sub–100-nm organic nanoparticles (NPs) combine useful features of ultrasmall size (11, 12), surface modification (13), controlled drug release, biodegradability, and biocompatibility (14). Liposomal, polymeric, and albumin-based NPs have been formulated to improve drug solubility and deliver paclitaxel at doses higher than otherwise possible in circulation (15–17). Temporal control of drug delivery may facilitate endothelial healing after injury, as NPs may be used to deliver antiproliferative agents to the vascular wall when neointimal proliferation is most active, followed by complete degradation and clearance (18). Targeted NPs that bind to exposed antigens in injured arteries may help to achieve therapeutic doses at sites of injury, because antiproliferative drugs such as paclitaxel have to be localized for action (19). In particular, systemic delivery of antiproliferative drugs to the specific site of disease remains an attractive goal, given the ease of drug administration (20).

Our initial work showed localization of a targeted NP system, termed nanoburrs, onto injured vasculature. The nanoburrs were designed with a lipid core-shell interface between poly(lactide-*co*-glycolic acid) (PLGA) and poly(ethylene glycol) (PEG) polymers (21, 22) and functionalized with heptameric peptides that were isolated in a M13 bacteriophage screen against collagen IV (23). Collagen IV, a heterotrimeric extracellular molecule, was chosen as the target because it represents 50% of the vascular basement membrane (24) and is exposed as a result of increased vascular permeability during injury and disease (25). Following systemic administration of fluorescently labeled nanoburrs in a rat carotid injury model, nanoburr localization to angioplastied arteries was 50% greater than with nontargeted NPs and twofold greater in angioplastied arteries than in healthy arteries (23).

In this study, we developed a systemically administered, paclitaxel-encapsulated, targeted NP system and evaluated its potential clinical utility by focusing on parameters of efficacy, tolerability, and pharmacokinetics in animal models. Based on the hypothesis that localization of antiproliferative drugs to injured vessels may result in improved drug potency and better treatment outcomes, we delivered paclitaxel-encapsulated nanoburrs as an i.v. bolus after balloon angioplasty in a rat carotid model. In vivo efficacy studies where the paclitaxel-encapsulated nanoburr formulations were given as equal i.v. doses on days 0 and 5 of surgery resulted in lower neointima-to-media (N/M) scores at 2 wk versus a standard paclitaxel formulation in solution, paclitaxel-encapsulated nontargeted NP, and sham, injury-only groups.

Results

Synthesis and Characterization of NP Treatment Groups. Nanoburrs with a core-shell lipid–polymeric structure and collagen IV-targeting peptides on the surface were formulated by nano-

Author contributions: J.M.C., J.-W.R., G.G., R.L., and O.C.F. designed research; J.M.C. and J.-W.R. performed research; J.M.C., J.-W.R., C.L.D., R.T.B., R.L., and O.C.F. analyzed data; and J.M.C., J.-W.R., R.L., and O.C.F. wrote the paper.

Conflict of interest statement: In compliance with the Brigham and Women's Hospital and Harvard Medical School institutional guidelines, O.C.F. discloses his financial interest in BIND Biosciences and Selecta Biosciences, two biotechnology companies developing nanoparticle technologies for medical applications. BIND and Selecta did not support the aforementioned research, and currently these companies have no rights to any technology or intellectual property developed as part of this research.

[1]J.M.C. and J.-W.R. contributed equally to this work.

[2]To whom correspondence may be addressed. E-mail: rlanger@mit.edu or ofarokhzad@zeus.bwh.harvard.edu.

This article contains supporting information online at www.pnas.org/lookup/suppl/doi:10.1073/pnas.1115945108/-/DCSupplemental.

precipitation and self-assembly (Fig. 1*A*) (23). The peptides were synthesized with a linker sequence (GGGC) at the C terminus for thiomaleimide coupling. Peptide affinity was characterized by site-specific binding competition of phage-displayed peptides against synthetic peptides on Matrigel, a basement membrane extract rich in collagen IV, to obtain a dose–response competition curve of IC_{50} = 114 nmol/L (23). NP sizes measured by dynamic light scattering were 55.1 ± 0.4 nm (polydispersity = 0.075, n = 3) after sterile filtration, with batch-to-batch variation under ± 5 nm. NPs functionalized with peptides (nanoburrs) did not show a significant size increase beyond 5 nm (Fig. 1*B*). Transmission electron micrograph (TEM) images obtained with 2 mg/mL nanoburrs stained with uranyl acetate solution showed that the particles were spherical, monodisperse, and in the 50-nm size range (Fig. 1*B*).

To determine the final drug loading based on a 5 wt% paclitaxel/PLGA input, NP batches (n = 3) were lyophilized to obtain the final PLGA polymer weight (80% of final mass; as the other 20% is lipid and PEG mass). After measuring drug content by RP-HPLC, the encapsulation efficiency was calculated to be 20% of the drug input weight, and the final drug load was determined to be ∼1% by paclitaxel/PLGA polymer weight. In comparison with previous studies where a burst release was observed with higher drug loading (21), a burst release was not observed at this paclitaxel load (Fig. 1*C*), likely due to overall reduced drug levels at the core-shell interface.

To measure drug release rates in vitro, NP samples were dialyzed in 3.5 L of PBS buffer at 37 °C and samples were withdrawn at indicated time points. The drug release half-life was determined to be ∼17.8 h for the nanoburrs and 18.2 h for the NP groups, which suggests that peptide conjugation only slightly interfered with the self-assembly process to marginally increase rates of drug release. For paclitaxel, a standard micellar formulation in Cremophor-EL/EtOH solution, the drug release half-life was found to be ∼10.5 h (Fig. 1*C*).

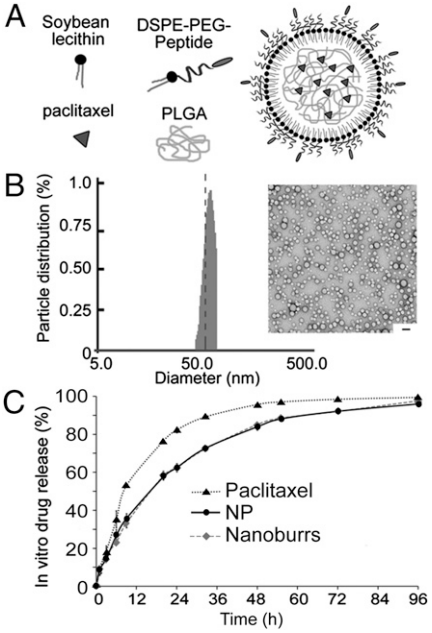

Fig. 1. Formulation and characterization of paclitaxel-encapsulated peptide-targeted NPs (nanoburrs). (*A*) Schematic of targeted lipid-polymeric NP design. The nanoburrs have a core-shell structure: soybean lecithin and peptide-conjugated distearoylphosphatidylethanolamine–poly(ethylene glycol) (DSPE–PEG–Peptide) form the shell; poly(lactic-coglycolic acid) (PLGA) encapsulating paclitaxel forms the core. (*B*) Dynamic light scattering plot showing the size ranges of nanoburrs. (*Inset*) Transmission electron micrograph (TEM) image of nanoburrs. (Scale bar, 100 nm.) (*C*) In vitro drug release studies with paclitaxel, NP, and nanoburr formulations. The graph shows percentage of drug release from samples placed in a PBS buffer sink at 37 °C with stirring.

Tolerability Studies. Maximum tolerated dose (MTD) studies were carried out in healthy Swiss albino mice comparing nanoburrs to paclitaxel using a single-dose i.v. injection. The Food and Drug Administration (FDA)-approved paclitaxel formulation uses Cremophor-EL as a solubilizing agent, but this formulation has been shown to cause neuropathy, complement activation, and hypersensitivity reactions, which necessitate steroid premedication (26). The paclitaxel MTD in experimental animals [paclitaxel (mg)/body weight (kg)] varies across studies; in our study, the paclitaxel MTD was found to be 10 mg/kg in mice, consistent with previous reports (27, 28). Doses of 15 mg/kg of paclitaxel caused the immediate death of two mice, possibly related to inadequate blood solubility at 1.2 mg/mL doses. In contrast, nanoburrs dosed at 35 mg paclitaxel/kg in mice (2.5 mg/mL concentrations in saline with 1% drug loading efficiency) were well tolerated, suggesting an advantage from improved drug solubility and NP compatibility. Higher doses were not given to avoid exceeding the maximum volume that can be safely injected as a bolus (∼10–15 mL/kg body weight). The animals were weighed daily and monitored for hair loss, vomiting, or diarrhea. The animals were also monitored for signs of tremors, staggering, and general responsiveness. At 10 mg/kg paclitaxel and 35 mg/kg nanoburrs, neither regimen caused adverse medical or behavioral effects, aside from very marginal body weight loss (<10% of initial mass). Blood samples were also collected at day 7 for biochemical and hematological analyses. The readings taken for the 10 mg/kg paclitaxel group indicated signs of mild thrombocytopenia (platelet count <400 K/μL) in two mice, but otherwise readings were within the expected range (Table 1). Likewise, neither regimen had significant effects on various biochemical parameters suggestive of hepatic and renal injury (Table 1). Upon study termination, gross necropsies and examination of histological cross-sections of major organs including the peripheral nerves gave no findings of toxicity.

Hence, we concluded that the paclitaxel-encapsulated nanoburr formulation was well tolerated in mice, with a ≥3.5-fold improvement in maximal tolerated dose versus paclitaxel. Considering that the intended doses for subsequent antiproliferative studies (≤1 mg/kg paclitaxel) were well within tolerability limits for i.v. administration, our MTD studies indicated the feasibility of efficacy trials using this biocompatible and biodegradable formulation.

Rat Carotid Injury Model Efficacy Studies. A rat carotid balloon-injury model was used to investigate the use of paclitaxel-encapsulated nanoburrs as a treatment for cellular proliferation after arterial injury. Balloon injury from repeated inflation and withdrawal of the balloon catheter induces endothelial cell loss and intimal damage. Although this is a standardized protocol for endothelial denudation, some media may also have been removed during the process, which is technically difficult to avoid. To prevent postprocedural acute thrombosis, rats were given a single dose of oral aspirin and i.v. heparin. Representative H&E-stained carotid artery cross-sections taken on day 0 of the surgery showed the loss of an endothelial monolayer from arterial balloon injury (Fig. 2*B*) compared with noninjured arteries (Fig. 2*A*). At 2 wk, Movat Pentachrome-stained cross-sections of balloon-injured left carotids showed extensive neointimal proliferation and luminal narrowing (Fig. 2*D*) compared with healthy right carotids (Fig. 2*C*).

Three treatment groups of paclitaxel, NP, and nanoburrs were compared against sham, injury-only groups. Paclitaxel samples were given as an i.v. bolus injection at either 0.3 mg/kg or 1 mg/kg,

Table 1. Hematological analysis and serum biochemical parameters from Swiss albino mice 168 h after a single i.v. dose

	Saline	Paclitaxel, 10 mg/kg	Nanoburrs, 35 mg/kg
RBC, M/μL	8.09 ± 0.676	8.30 ± 0.598	7.94 ± 0.512
HGB, g/dL	13.7 ± 1.11	14.2 ± 0.796	13.5 ± 0.685
HCT, %	49.0 ± 3.19	49.3 ± 2.63	46.9 ± 1.78
MCV, fL	60.6 ± 1.95	59.5 ± 1.55	59.2 ± 2.51
MCH, pg	16.8 ± 0.386	17.1 ± 0.679	17.0 ± 0.629
MCHC, g/dL	27.9 ± 0.592	28.8 ± 0.750	28.7 ± 0.882
PLT, K/μL	1395 ± 42.1	1026 ± 533	1415 ± 514
WBC, K/μL	2.03 ± 0.677	2.05 ± 0.454	3.79 ± 0.741
Neut, %	0.28 ± 0.167	0.231 ± 0.227	0.278 ± 0.185
Lymph, %	86.8 ± 17.2	68.9 ± 12.9	77.4 ± 15.6
Mono, %	3.70 ± 4.70	16.7 ± 6.38	11.4 ± 7.15
Eo, %	0.185 ± 0.230	0.226 ± 0.427	0.124 ± 0.146
Baso, %	9.03 ± 12.5	14.0 ± 7.77	10.78 ± 8.90
ALP, U/L	39.8 ± 3.24	41.7 ± 1.77	43.6 ± 2.73
AST, U/L	109.50 ± 11.22	119.83 ± 8.23	114.67 ± 12.51
ALT, U/L	65.23 ± 10.40	61.01 ± 6.10	66.10 ± 4.47
BUN, mmol/L	8.40 ± 1.48	8.31 ± 1.61	7.98 ± 1.55

Results are expressed as mean ± SD, $n = 6$. Units of mg/kg represent the active drug composition. RBC, red blood cells; HGB, hemoglobin; HCT, hematocrit; MCV, mean cell volume; MCH, mean cell hemoglobin; MCHC, mean cell hemoglobin concentration; PLT, platelets; WBC, white blood cells; Neut, neutrophils; Lymph, lymphocytes; Mono, monocytes; Eos, eosinophils; Baso, basophils; ALP, alkaline phosphatase; AST, aspartate aminotransferase; ALT, alanine aminotransferase; BUN, blood urea nitrogen.

with five animals per treatment dose. Repeat dosing is noninvasive and may be beneficial in preventing neointimal proliferation (29). To determine the optimal timing for a repeat dose, in vivo pharmacokinetic studies of nanoburrs were performed (Fig. S1). Nanoburr levels tracked by ^{3}H–PLGA were detected as late as 120 h, whereas paclitaxel levels tracked by ^{14}C–paclitaxel could not be further detected after 24 h, likely due to concurrent drug release in circulation. Given these parameters, we selected day 5 for the repeat dose to avoid stacked drug dosing, because circulatory and arterial tissue levels of both carrier and drug would be clinically insignificant by 120 h. Subsequently, all treatment groups were given two equal doses postangioplasty on day 0 and day 5, midway to the conclusion of the study. The surgical procedure itself and sample dosing did not cause mortality or any apparent morbidity. The mean weights of animals were measured daily; Table S1 shows the average weights of each treatment group at day 0 (preprocedure), day 7, and day 14. During the study, all animals including sham-operated animals lost up to 5% of their original mean body weight at day 7 and gained 10% of their original mean body weight by day 14 (all versus day 0).

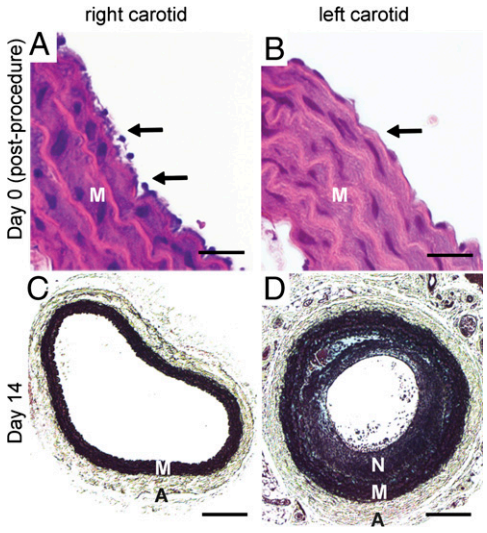

Fig. 2. Histological progression of balloon-injured carotid artery lesions. (*A*) Normal right carotid artery wall. Note the very thin intima (arrows) overlying the media. (*B*) Balloon-injured left carotid artery wall taken immediately after injury shows the absence of an endothelial layer in the intima (arrow). (*C*) Arterial cross-section of a normal right carotid artery at day 14. (*D*) In contrast, arterial cross-section of an untreated balloon-injured carotid artery at day 14 shows a markedly thickened intima that contains large amounts of collagen (light blue) and elastin (blue-black). Images were obtained with a Zeiss microscope using the 5× objective. N, neointima; M, media; A, adventitia. (*A* and *B*) H&E staining. (Scale bar, 20 μm.) (*C* and *D*) Movat Pentachrome staining. (Scale bar, 200 μm.)

At 2 wk, animals were killed and both the right (noninjured) and the left (angioplastied) carotids were harvested for morphometric quantification using ImageJ software (National Institutes of Health, NIH). The degree of neointimal thickening was denoted as a unitless ratio of N/M area (Table 2). N/M measurements were taken from the site of greatest luminal narrowing per artery, as this is the standard of the field and the most clinically relevant (19, 30).

We ensured that there was minimal procedural variation in our study, and this was consistent with our observations that the sham, injury-only group exhibited the highest N/M ratio with a SD of <5% (~3.7%) of the average ratio ($N/M_{sham,\ injury\ only}$ = 1.249 ± 0.046). Compared with the sham, injury-only group, all treatment groups at a 1 mg/kg dose (paclitaxel, NPs, and nanoburrs) resulted in significant reduction of N/M ratios ($P < 0.01$, all versus sham, injury-only group). The greatest reduction was observed with the nanoburr group ($N/M_{nanoburr}$ = 0.662 ± 0.169, $P < 0.01$ versus sham, injury-only group). Similarly, with doses lowered threefold to 0.3 mg/kg, the nanoburr group resulted in the lowest N/M ratio ($N/M_{nanoburr}$ = 0.744 ± 0.129, $P < 0.01$ versus sham, injury-only group). To a lesser degree, the paclitaxel group also resulted in significant reduction ($N/M_{paclitaxel}$ = 0.937 ± 0.126, $P < 0.05$ versus sham, injury-only group). Subsequent comparison of the efficacy of nanoburr (targeted) and NP (nontargeted) treatments showed a trend toward an improved N/M ratio at 0.3 mg/kg doses ($N/M_{nanoburr}$ = 0.744 ± 0.129 versus N/M_{NP} = 1.063 ± 0.097, $P = 0.08$). The antistenotic efficacy observed with low therapeutic doses indicates improved potency of paclitaxel treatment by nanoburr localization to the site of injury.

Representative images taken with H&E staining show qualitative differences in neointima (N) thickness in relation to the media (M) and versus sham, injury-only saline groups (Fig. 3). The neointimal proliferation seen here shows a dose–response relationship when high and low doses of paclitaxel are given, and when targeting is added, in particular at 1 mg/kg doses.

Cross-sections of the harvested arteries were then stained with α-smooth muscle actin (α-SMA) antibodies to compare the de-

Table 2. N/M ratio measurements of intimal proliferation

Treatment	High dose (1 mg/kg)	Low dose (0.3 mg/kg)
Sham, injury only (saline)	1.249 ± 0.046	—
Paclitaxel	0.837 ± 0.087†	0.937 ± 0.126*
NP	0.749 ± 0.136†	1.063 ± 0.097
Nanoburrs	0.662 ± 0.169†	0.744 ± 0.129†,‡

N/M ratios taken from the site of greatest luminal narrowing per artery. Doses indicate active paclitaxel drug composition. Animals were dosed on days 0 and 5 postsurgery and the study was concluded on day 14. All results are expressed as mean ± SEM, $n = 5$. *$P < 0.05$ versus injury only; $^{\dagger}P < 0.01$ versus sham, injury-only; $^{\ddagger}P = 0.08$ versus NP, by one-way ANOVA with Tukey's post hoc test.

gree of neointimal formation across the groups. Experimental conditions were optimized to show differential staining of neointima among the tested groups. Consequently, uninjured arteries representing baseline media without significant neointima stained weakly for α-SMA (Fig. 4*A*), whereas nontreated, injured arteries (Fig. 4*B*) and injured arteries in the low-dose groups (Fig. 4 *C*, *E*, and *G*) stained dark brown, indicating dynamic neointimal formation. Overall, the nanoburr-treated groups showed improved lumen patency and reduction in α-SMA staining (Fig. 4*H*) compared with other high-dose groups (Fig. 4 *D* and *F*).

Finally, four major organs from each experimental animal were harvested on day 14 and H&E stained for histological evaluation (Fig. 5). Studies have shown that histological evidence of organ toxicity can be observed postinjection within days (31, 32). In this study, a thorough examination of H&E-stained organ sections did not reveal any significant signs of toxicity.

Discussion

In this study, we show that the delivery of paclitaxel-encapsulated nanoburrs to injured vessels is effective in suppressing stenosis. Considering recent developments in DES design (33) and longer-term clinical safety reports (34, 35), we envision that the nanoburrs may be useful for a subset of patients who are currently unable to receive DESs. This group may have preexisting comorbidities, planned surgeries, or lesions not amenable for stenting (longer lesions, branch points, and diffusely diseased, smaller arteries) (2). For patients who have received DESs or BMSs, the nanoburrs may potentially be used in conjunction to maintain long-term patency. They may also find use in plain old balloon angioplasty procedures (POBA). Finally, the nanoburrs may potentially be used in early stage CAD to deliver antiinflammatory treatments to prestenotic lesions (36).

Collagen IV was chosen as a target for drug delivery because a pronounced accumulation of extracellular matrix is observed as the neointima grows (7). During this modulation process, the SMC in the neointima undergoes a phenotypic change from contractile to synthetic. In one study with balloon-injured Sprague-Dawley rats, a 50% increase in collagen mass was deposited along the injured arteries after 1 wk (37). Hence, neointimal formation appears to correlate well with increased collagen levels, making collagen IV an excellent candidate for targeting injured arteries. Because the animals were also given a repeat dose on day 5, increased collagen deposition may contribute to the antistenotic efficacy observed here. Effective repeat dosing that corresponds to lesion severity may be useful for chronic diseases like atherosclerosis (19, 29), which may not always be resolved by revascularization alone (20).

Paclitaxel-encapsulated nanoburrs may have a number of advantages over the standard micellar formulation of paclitaxel (Taxol) as shown in this study. Whereas Taxol, an FDA-approved formulation for systemic paclitaxel delivery, has been associated with various side effects that narrow its therapeutic window (26), the nanoburrs were shown to have a ≥3.5-fold improved maximum tolerated dose over Taxol in safety studies. Also, their prolonged circulatory half-life may enhance retention at sites where permeability is enhanced (33). Furthermore, the ability to surface functionalize NPs means that not only peptides, but other types of targeting ligands such as antibodies and small molecules may be added to improve drug delivery to sites of vascular injury.

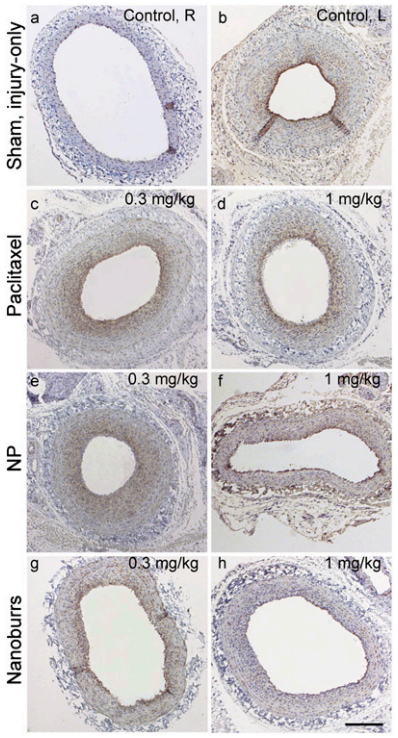

Fig. 4. Immunohistochemical staining for α-smooth muscle actin (SMA). (*A* and *B*) Sham, injury-only groups received angioplasty to the left artery. High intensity of SMA-stained cells and a cellular neointimal cap was observed in an angioplastied left artery. No specific staining was observed in a non-angioplastied right artery. (*C* and *D*) Angioplastied left arteries representative of paclitaxel-treated groups at two treatment doses. (*E* and *F*) Angioplastied left arteries representative of NP-treated groups at two treatment doses. (*G* and *H*) Angioplastied left arteries representative of nanoburr-treated groups at two treatment doses. (Scale bar for all images, 200 μm.)

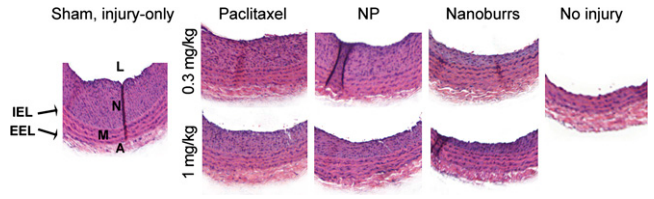

Fig. 3. Representative H&E-stained sections from different treatment groups. Images were obtained with a Zeiss microscope using the 5× objective. Note the difference in lumen patency between different doses of the same treatment group and also compared with sham, injury-only groups. L, lumen; N, neointima; M, media; A, adventitia; IEL, internal elastic lamina; EEL, external elastic lamina.

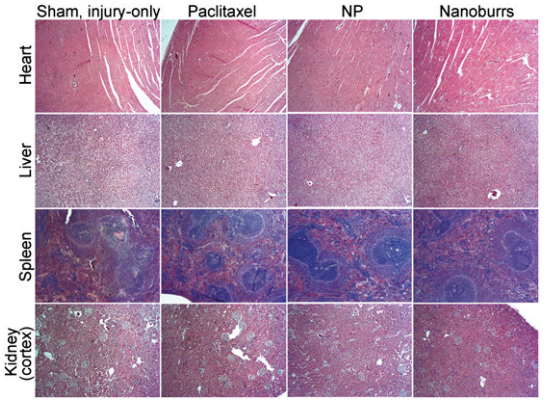

Fig. 5. H&E-stained sections of rat organs after i.v. administration of saline, paclitaxel, NP, or nanoburrs on days 0 and 5 postsurgery in Sprague-Dawley rats. Treatments were given at 1 mg/kg active drug composition. Images were obtained with a Zeiss microscope using the 5× objective.

Previous biodistribution studies in our laboratory have shown a common profile of ~60–80% of the polymeric nanoparticles being taken up by the mononuclear phagocytic system (MPS, formerly termed the reticuloendothelial system), and a small fraction (<5%) being localized at a site of interest (38). Thus, we estimate that ~1–3% of the NPs would be captured in the injured artery, with nanoburrs localizing at the injury about twice more than at a noninjured artery. Given the limited availability of prior data, it is difficult to compare therapeutic systemic doses of paclitaxel in rats for preventing arterial stenosis. However, the doses used in this efficacy study (0.3 mg/kg and 1 mg/kg) appear to be comparable to, or lower than, previous studies (19, 39).

The statistical significance obtained with the nanoburr treatment group against the sham, injury-only group ($P < 0.01$ versus sham, injury-only) suggests the efficacy of nanoburr treatment at both high and low doses. We also observed a clear trend of improvement with the nanoburr treatment versus other treatments (nontargeted NPs and paclitaxel). Notably, at low-dose treatments (0.3 mg/kg), there was an ~30% greater reduction in arterial stenosis with nanoburr treatment compared with nontargeted NP treatment ($P = 0.08$, $N/M_{nanoburr}$ versus N/M_{NP}). This trend was less obvious with high-dose treatments (1 mg/kg) as all groups tend toward improved N/M scores, making statistical significance difficult to measure between groups. While it is believed that further dose reduction will accentuate differences between groups, the neointimal reduction obtained in our efficacy studies are otherwise comparable to Kolodgie et al. (19), which demonstrated treatment in a stented rabbit model using albumin-stabilized paclitaxel (Coroxane). Whereas Kolodgie et al. delivered paclitaxel via intraarterial infusion, our work is a systemically delivered, locally acting paclitaxel therapy for the treatment of arterial stenosis, which requires additional consideration of whole-body pharmacokinetics. Overall, this study involved overlapping parameters of pharmacokinetic profiles, drug release kinetics, dosing frequencies, and targeting ligand densities, which all need to be controlled in tandem and lead to complexity in interpreting our results.

One of the biggest differences between the rat carotid artery angioplasty model versus human atheromatous lesions is the absence of underlying atheroma in the angioplasty model. Whereas in our system the efficacy of the nanoburr platform is advanced by simple exposure to collagen, the presence of underlying atheroma with subsequent angioplasty in clinical application may result in a higher thrombogenic potential, providing an obscuring factor for peptide binding. The inherent thrombogenecity of intralesional components such as necrotic lipid and tumor necrosis factor may alter the application of targeted NPs as well. However, the rat carotid model is a well-defined model, which is appropriate for this proof-of-concept work. Further studies to investigate the efficacy of nanoburrs in an experimental atherosclerotic model will be useful.

Previously, we used paclitaxel–poly(lactic acid) drug conjugates that show extended elution rates of approximately 1 wk in vitro (23). In this study, however, we used unconjugated paclitaxel to directly compare paclitaxel-encapsulated nanoburr potency against free paclitaxel administered in its conventional form. Paclitaxel, once released from the circulating nanoburrs, is subject to a similar pharmacokinetic profile as with Taxol. The nanoburrs themselves, however, have a longer circulation half-life, which may effectively prolong drug circulation when used with paclitaxel–polymer conjugates. Hence, the combination of targeting with slow-eluting paclitaxel conjugates may further improve on the antistenotic effect shown here. Longer-term studies may also accentuate the contribution of very slow-eluting NP medicines. Beyond paclitaxel, the variety of antiproliferative treatments can be expanded to sirolimus and its analogs, newer developed drugs (40), and combination treatments.

In conclusion, targeted NP delivery of antiproliferative therapies, given as a two-dose infusion on days 0 and 5 of injury, effectively prevented arterial stenosis with an ~50% reduction in N/M ratio compared with the sham-injury group. Our findings indicate that the nanoburrs may have potential clinical benefits as a systemically delivered treatment for injured vasculature. This NP-based therapy combines effective vascular targeting and controlled drug release to achieve its efficacy, independent of arterial anatomy or stent placement.

Materials and Methods

A detailed description is available in *SI Materials and Methods*.

Synthesis and In Vitro Characterization of Nanoburrs. The nanoburrs were synthesized as previously described (23), with materials and modifications noted in *SI Materials and Methods*. ^{14}C–paclitaxel- and ^{3}H–PLGA-labeled nanoburrs were prepared by adding radiolabeled material to acetone-solubilized PLGA before nanoprecipitation. Nanoburrs were characterized using standard protocols (22).

Animals. Animal studies were conducted by a certified contract research organization. All animal studies were carried out using protocols consistent with local, state, and federal regulations as applicable and approved by the institutional animal care and use committee.

Formulation Tolerability Studies. A total of 54 male Swiss albino mice weighing ~25–30 g were obtained from Charles River Laboratories. Mice were used in these studies for ease of dose escalation and availability of literature values. A single preparation was used for each formulation, i.e., 2.5 mg/mL nanoburrs and 1.2 mg/mL paclitaxel based on the active drug composition. Paclitaxel in solution was prepared as previously described (41) in a 1/1 volume ratio of CrEL and USP-grade EtOH, diluted in saline to 0.3–1.2 mg/mL and sterile filtered. Animals were given a single i.v. bolus dose via the tail vein ($n = 4$ per group). After 7 d of clinical monitoring, the animals were killed by CO_2 inhalation for gross necropsy of the major organs (liver, lung, heart, spleen, kidney, and peripheral nerves). In a parallel study, blood samples ($n = 6$ per group) were taken at day 7 for hematological analysis and assessment of biochemical parameters.

Rat Carotid Injury Model and Neointimal Proliferation Studies. Thirty-five male Sprague-Dawley rats weighing ~450 g were obtained from Charles River Laboratories. Animals were given aspirin (20 mg/kg) by oral gavage and heparin (250 IU/kg) by i.v. injection immediately before surgery. Animals were anesthetized intramuscularly (i.m.) with ketamine (60 mg/kg)/xylazine (10 mg/kg) and given buprenorphine as an analgesic. Rat carotid injury was performed as previously described (42). Immediately after ligation of the arteriotomy site, samples were i.v. injected into the tail vein. A second equal i.v. dose was given on day 5. At 2 wk, animals were killed by CO_2 inhalation. H&E- and Movat Pentachrome-stained sections of major organs were examined and both carotids were harvested for computerized morphometric analysis.

Histological Morphometric Analysis. Nine H&E-stained carotid sections per artery were imaged with a Zeiss microscope under the bright-field setting using the 5× objective. ImageJ software (NIH) was used to assess all sections by an investigator blinded to the experimental samples. The degree of neointimal thickening was expressed as a ratio between the neointimal (N) and medial (M) areas, with the highest cross-sectional N/M score representing the site of greatest narrowing assigned to each artery. This site may not necessarily reside at the midpoint of the artery but is most clinically relevant.

Immunohistochemistry Studies. Immunohistochemistry of α-smooth muscle actin (SMA) was carried out using standard protocols (43) with antibodies raised against α-SMA (Dako).

ACKNOWLEDGMENTS. This study was supported in part by National Cancer Institute Grant CA151884 (to R.L. and O.C.F.), National Institute of Biomedical Imaging and Bioengineering Grant EB003647 (to O.C.F.), National Heart, Lung, and Blood Institute Program of Excellence in Nanotechnology Award, Contract #HHSN268201000045C (to R.L. and O.C.F.), and the David H. Koch–Prostate Cancer Foundation Award in Nanotherapeutics (R.L. and O.C.F.). The authors acknowledge financial support from the Singapore Agency for Science, Technology and Research Fellowship (J.M.C.), the Howard Hughes Medical Institute Medical Fellows Program (J.-W.R.), and the Burroughs Wellcome CAMS Award (to C.L.D.).

1. Serruys PW, Kutryk MJ, Ong AT (2006) Coronary-artery stents. *N Engl J Med* 354: 483–495.
2. Mehran R, Dangas GD (2007) Off-label use of drug-eluting stents: Assessing the risk. *Nat Clin Pract Cardiovasc Med* 4:594–595.
3. Finn AV, et al. (2007) Vascular responses to drug eluting stents: Importance of delayed healing. *Arterioscler Thromb Vasc Biol* 27:1500–1510.
4. Windecker S, Meier B (2007) Late coronary stent thrombosis. *Circulation* 116: 1952–1965.
5. Stone GW, et al. (2007) Safety and efficacy of sirolimus- and paclitaxel-eluting coronary stents. *N Engl J Med* 356:998–1008.
6. Ducrocq G, Serebruany V, Tanguay JF (2007) Antiplatelet therapy in the era of drug-eluting stents: Current and future perspectives. *Expert Rev Cardiovasc Ther* 5:939–953.
7. Schwartz SM, deBlois D, O'Brien ER (1995) The intima. Soil for atherosclerosis and restenosis. *Circ Res* 77:445–465.
8. Farb A, et al. (1999) Pathology of acute and chronic coronary stenting in humans. *Circulation* 99:44–52.
9. Lanza G, et al. (2006) Nanomedicine opportunities in cardiology. *Ann N Y Acad Sci* 1080:451–465.
10. Godin B, et al. (2010) Emerging applications of nanomedicine for the diagnosis and treatment of cardiovascular diseases. *Trends Pharmacol Sci* 31:199–205.
11. Fishbein I, et al. (2001) Formulation and delivery mode affect disposition and activity of tyrphostin-loaded nanoparticles in the rat carotid model. *Arterioscler Thromb Vasc Biol* 21:1434–1439.
12. Westedt U, et al. (2002) Deposition of nanoparticles in the arterial vessel by porous balloon catheters: Localization by confocal laser scanning microscopy and transmission electron microscopy. *AAPS PharmSci* 4:E41.
13. Labhasetwar V, Song C, Humphrey W, Shebuski R, Levy RJ (1998) Arterial uptake of biodegradable nanoparticles: Effect of surface modifications. *J Pharm Sci* 87: 1229–1234.
14. Zhang L, et al. (2008) Nanoparticles in medicine: Therapeutic applications and developments. *Clin Pharmacol Ther* 83:761–769.
15. Brito L, Amiji M (2007) Nanoparticulate carriers for the treatment of coronary restenosis. *Int J Nanomedicine* 2:143–161.
16. Chorny M, et al. (2010) Targeting stents with local delivery of paclitaxel-loaded magnetic nanoparticles using uniform fields. *Proc Natl Acad Sci USA* 107:8346–8351.
17. Kolodgie FD, et al. (2002) Sustained reduction of in-stent neointimal growth with the use of a novel systemic nanoparticle paclitaxel. *Circulation* 106:1195–1198.
18. Labhasetwar V, Song CX, Levy RJ (1997) Nanoparticle drug delivery system for restenosis. *Adv Drug Deliv Rev* 24:63–85.
19. Axel DI, et al. (1997) Paclitaxel inhibits arterial smooth muscle cell proliferation and migration in vitro and in vivo using local drug delivery. *Circulation* 96:636–645.
20. Sirois MG, Simons M, Kuter DJ, Rosenberg RD, Edelman ER (1997) Rat arterial wall retains myointimal hyperplastic potential long after arterial injury. *Circulation* 96: 1291–1298.
21. Zhang L, et al. (2008) Self-assembled lipid—polymer hybrid nanoparticles: A robust drug delivery platform. *ACS Nano* 2:1696–1702.
22. Chan JM, et al. (2009) PLGA-lecithin-PEG core-shell nanoparticles for controlled drug delivery. *Biomaterials* 30:1627–1634.
23. Chan JM, et al. (2010) Spatiotemporal controlled delivery of nanoparticles to injured vasculature. *Proc Natl Acad Sci USA* 107:2213–2218.
24. Hudson BG, Reeders ST, Tryggvason K (1993) Type IV collagen: Structure, gene organization, and role in human diseases. Molecular basis of Goodpasture and Alport syndromes and diffuse leiomyomatosis. *J Biol Chem* 268:26033–26036.
25. Ross R (1999) Atherosclerosis—an inflammatory disease. *N Engl J Med* 340:115–126.
26. Gelderblom H, Verweij J, Nooter K, Sparreboom A (2001) Cremophor EL: The drawbacks and advantages of vehicle selection for drug formulation. *Eur J Cancer* 37: 1590–1598.
27. Hureaux J, et al. (2010) Toxicological study and efficacy of blank and paclitaxel-loaded lipid nanocapsules after i.v. administration in mice. *Pharm Res* 27:421–430.
28. Kim SC, et al. (2001) In vivo evaluation of polymeric micellar paclitaxel formulation: Toxicity and efficacy. *J Control Release* 72:191–202.
29. Uwatoku T, et al. (2003) Application of nanoparticle technology for the prevention of restenosis after balloon injury in rats. *Circ Res* 92:e62–e69.
30. Danenberg HD, et al. (2003) Liposomal alendronate inhibits systemic innate immunity and reduces in-stent neointimal hyperplasia in rabbits. *Circulation* 108:2798–2804.
31. Pereverzeva E, et al. (2008) Intravenous tolerance of a nanoparticle-based formulation of doxorubicin in healthy rats. *Toxicol Lett* 178:9–19.
32. Al-Jamal KT, et al. (2010) Systemic antiangiogenic activity of cationic poly-L-lysine dendrimer delays tumor growth. *Proc Natl Acad Sci USA* 107:3966–3971.
33. Kukreja N, Onuma Y, Daemen J, Serruys PW (2008) The future of drug-eluting stents. *Pharmacol Res* 57:171–180.
34. Stone GW, et al.; HORIZONS-AMI Trial Investigators (2009) Paclitaxel-eluting stents versus bare-metal stents in acute myocardial infarction. *N Engl J Med* 360:1946–1959.
35. James SK, et al.; SCAAR Study Group (2009) Long-term safety and efficacy of drug-eluting versus bare-metal stents in Sweden. *N Engl J Med* 360:1933–1945.
36. Libby P, Theroux P (2005) Pathophysiology of coronary artery disease. *Circulation* 111: 3481–3488.
37. Nili N, Zhang M, Strauss BH, Bendeck MP (2002) Biochemical analysis of collagen and elastin synthesis in the balloon injured rat carotid artery. *Cardiovasc Pathol* 11: 272–276.
38. Gu F, et al.; (2008) Precise engineering of targeted nanoparticles by using self-assembled biointegrated block copolymers. *Proc Natl Acad Sci USA* 105:2586–2591.
39. Sollott SJ, et al.; (1995) Taxol inhibits neointimal smooth muscle cell accumulation after angioplasty in the rat. *J Clin Invest* 95:1869–1876.
40. Kim SY, et al. (2009) Activation of NAD(P)H:quinone oxidoreductase 1 prevents arterial restenosis by suppressing vascular smooth muscle cell proliferation. *Circ Res* 104: 842–850.
41. Gelderblom H, et al. (2002) Influence of Cremophor El on the bioavailability of intraperitoneal paclitaxel. *Clin Cancer Res* 8:1237–1241.
42. Tulis DA (2007) Rat carotid artery balloon injury model. *Methods Mol Med* 139:1–30.
43. Cohen-Sela E, et al. (2006) Alendronate-loaded nanoparticles deplete monocytes and attenuate restenosis. *J Control Release* 113:23–30.